



HAL
open science

Dynamic measurement of the airflow rate in a two-zones dwelling, from the CO₂ tracer gas-decay method using the Kalman filter

Gabriel Remion, Bassam Moujalled, Mohamed El Mankibi

► To cite this version:

Gabriel Remion, Bassam Moujalled, Mohamed El Mankibi. Dynamic measurement of the airflow rate in a two-zones dwelling, from the CO₂ tracer gas-decay method using the Kalman filter. *Building and Environment*, 2021, 188, pp.107493 -. 10.1016/j.buildenv.2020.107493 . hal-03492832

HAL Id: hal-03492832

<https://hal.science/hal-03492832>

Submitted on 15 Dec 2022

HAL is a multi-disciplinary open access archive for the deposit and dissemination of scientific research documents, whether they are published or not. The documents may come from teaching and research institutions in France or abroad, or from public or private research centers.

L'archive ouverte pluridisciplinaire **HAL**, est destinée au dépôt et à la diffusion de documents scientifiques de niveau recherche, publiés ou non, émanant des établissements d'enseignement et de recherche français ou étrangers, des laboratoires publics ou privés.



Distributed under a Creative Commons Attribution - NonCommercial 4.0 International License

Dynamic measurement of the airflow rate in a two-zones dwelling, from the CO₂ tracer gas-decay method using the Kalman filter

Gabriel Remion^{1 2*}, Bassam Moujalled¹, Mohamed El Mankibi²

¹ Cerema, Project-team BPE, 46 Rue St Théobald, L'isle d'Abeau, F-38081, France

² ENTPE – University of Lyon, LTDS, 3 rue Maurice Audin, Vaulx-en-Velin, 69120, France

*Corresponding author :

E-mail address : gabriel.remion@entpe.fr

Tel: +33 4 74 27 51 13

Abstract

The measurement of natural airflows is challenging, because of low pressures involved in natural ventilation, and because of their variability. The tracer gas decay method is the most used method to assess natural airflows. It is, however, not adapted to multi-zone dwellings. A protocol based on the decay method is tested here involving the Kalman filter, and a correction procedure of concentrations. Both intend to allow the measurement of the global airflow-rate of a multi-zone passive-stack ventilated dwelling. The correction procedure of concentrations inhibits infiltrations that would have an impact on the accuracy of the tracer decay method implemented in a multi-zone dwelling. The Kalman filter allows measuring a dynamic airflow-rate, while the background tracer gas concentration varies which would bias the conventional decay method. It is a key issue when implementing the CO₂ decay method in a multi-zone dwelling as, depending on its sources, the CO₂ concentration in any room of the dwelling is likely to vary. The robustness of the proposed protocol was tested through a parametrical analysis in laboratory twincells and it showed a significantly lower sensitivity

compared to the conventional 2-points decay method. Maximum deviations on the airflow-rate were systematically lower from 4 to 11 points. The concentration correction procedure allowed increasing the accuracy up to 190 points. The ability of the Kalman filter to assess the dynamic airflow-rate was questioned. It was strongly influenced by the process noise variance associated to state parameters of the Kalman filter, which are defined by the experimenter.

Keywords

Concentration-decay method; Kalman filter; Dynamic AER measurement.

Nomenclature

λ	Air Exchange Rate [vol.h ⁻¹]
λ_2	Air Exchange Rate calculated by the 2-points method [vol.h ⁻¹]
C	Inside concentration [ppm]
C_i	Initial concentration [ppm]
C_f	Final concentration [ppm]
C^*	Measured inside concentration [ppm]
C_{bg}	Background concentration [ppm]
C_{bg}^*	Measured background concentration [ppm]
C_{amb}^*	Measured ambient concentration [ppm]
v	Measurement noise [ppm]
V	Measurement noise variance matrix
w_λ	Process noise of the AER [vol.h ⁻²]
w_C	Process noise associated to the inside concentration [ppm.h ⁻¹]
$w_{C_{bg}}$	Process noise associated to the background concentration [ppm.h ⁻¹]
R	Process noise variance matrix
x	State-space
y	Output-space
u	Command-space
A	Transition matrix
C	Observation matrix
t_f	Final time [h]
t_i	Initial time [h]
τ	Time constant [h]
N	Number of measurement points [-]
σ_λ	Global uncertainty [%]
ε_λ	Deviation of the AER [%]

S_{ε}	Standard-deviation of the AER [%]
Q	Volumetric AER [$\text{m}^3 \cdot \text{h}^{-1}$]
A_{eff}	Effective area [m^2]
U_{buo}	Air speed induced by buoyancy forces [$\text{m} \cdot \text{h}^{-1}$]
U_{wind}	Air speed induced by the wind [$\text{m} \cdot \text{h}^{-1}$]
ΔP_{int}	Pressure differential [Pa]
ρ_{int}	Internal density [$\text{kg} \cdot \text{m}^{-3}$]
g	Acceleration of gravity [$\text{m} \cdot \text{s}^{-2}$]
H	Height between the air inlet and the air outlet [m]
ΔT	Temperature differential [$^{\circ}\text{C}$]
T_{int}	Internal temperature [$^{\circ}\text{C}$]
U	Wind speed [$\text{m} \cdot \text{s}^{-1}$]
ΔC_p	Pressure coefficient differential [-]

1. Introduction

1.1. Background on the measurement of natural airflows

Measuring natural airflows has always been a challenging task, especially in multi-room dwellings [1]–[3]. As an example, low pressure involved in natural ventilation systems prevent from using an airflow-meter, which would introduce a pressure drop, affecting the flow pattern. In addition, when dealing with natural airflow through large openings, airflow-meters can not be used without changing the cross section of the opening. Through a comprehensive study, Remion et al. [3] identified tracer gas measurement methods as being the most used methods to characterize natural airflows. According to the same study, the concentration decay method, compared to the constant dosing and the constant concentration tracer gas methods, appears to be the most suitable method for the in-situ assessment of natural ventilation's performance for several reasons:

- The constant concentration method is too sophisticated in terms of equipment and the expertise that it requires. In-situ applications were found in the literature [1], [4], but the constant concentration method is more restricted to research projects.
- Standards prerequisites describing the application of tracer gas methods [5], [6], impose to inject the gas homogeneously inside the tested building. For the constant

dosing and the constant concentration methods, which calculate the airflow rate using the gas injection rate, the injection shall be performed either with several dosing points, or with one dosing point associated with the use of a mixing fan. However, the mixing fan option should be avoided as it would alter the natural airflow path, and the implementation of several dosing point is not convenient for in-situ applications.

Tracer decay methods look to be alternative solutions. Indeed, they consist in dosing the gas before the beginning of the airflow measurement. The mixing fan is used during the injection process only and has no impact on the airflow measurement [5].

- Decay methods do not necessarily require a mass-flow controller.
- Decay methods can perform simultaneously the measurement of the age of air, and the airflow rate for natural ventilation systems [7], [8]. Both indicators jointly considered allow characterizing the ventilation efficiency, described by Sandberg [9]. The measurement of the age of air described by Roulet & Vandaele [8] can be performed also by the constant dosing strategy, but this requires to have an identified outlet opening, which is not necessarily the case for natural ventilation systems in real buildings.

Concerning its accuracy, it should be noticed that the concentration decay can be analysed through two sub-methods, the 2-points method, or the multi-points method [10]. The difference between both methods is that the 2-points method uses only two measurement points, increasing its sensibility to measurement noise, but allowing the airflow to be variable, while the multi-points method performs a least-squares regression reducing the sensibility towards measurement noise, but assuming a stationary airflow [10]. The comparative analysis of their accuracy based on the state-of-the-art led to similar values around 15% when implemented in natural ventilated buildings [3].

1.2. In-situ constraints for a multi-room dwelling

In-situ applications in naturally ventilated dwellings of tracer gas measurement add several constraints. Tracer gas methods with a single-tracer gas are not adapted to multi-zone buildings [5]. A multi-zone dwelling implies air inlets in each living room, and air outlets in each service room. The air is distributed from rooms containing inlets to rooms containing outlets. It flows from one room to another by means of transfer air components such as door undercuts, or transfer grills. The global Air Exchange Rate (AER) of a multi-zone building can be measured by performing the tracer gas method simultaneously in each exhaust room, or in each living room. The air recirculation would considerably alter the accuracy of the method performed in each living rooms, because the experimenter would assume that all the air coming to the living room comes from the outside. As the concentration of the recirculated air would significantly differ from the outside concentration, the method would not be reliable. Regarding exhaust rooms, if the tracer gas is present in the atmosphere, its concentration in the air coming to the room in which the tracer gas method is realised has to be subtracted to the inside concentration. As long as the concentration of the air coming from the rest of the dwelling is measured, the pattern of the upstream air has no influence. Furthermore, volumes of service rooms are likely to be smaller than living rooms' volumes, enhancing the homogeneity potential of the tracer gas, which is a prerequisite of those methods [5], [6]. Performing the method in service rooms still brings some constraints.

CO₂ as a tracer gas has progressively replaced SF₆ thanks to its low cost, to its lower environmental impact, and to the flourishing of cost-effective wireless CO₂ sensors that ease up the implementation in in-situ buildings [2]. It meets ideal tracer gas prerequisites, except the one mentioning that the tracer gas should not be present in the atmosphere. Its suitability as a tracer gas, though, has been proven compared to SF₆ results [11]. To bypass the prerequisite that imposes that the tracer gas should not be present in the atmosphere,

the concentration of the air coming to the tested room shall be subtracted to the inside concentration. This concentration is called the background concentration. It leads to two main constraints for multi-zone applications:

- An exhaust ventilation system installed in a dwelling is designed to drive the air from living rooms to service rooms by transfer air components. Thus, the straightforward mean to assess the background concentration, is to perform a measurement upstream the transfer air component that is connected to the service room. This measured concentration will be called “ambient concentration”. Yet, the background concentration is different from the ambient concentration in case of any infiltration to the service room. Assuming the ambient concentration to be the background concentration may lead to significant discrepancies.
- Tracer gas methods are biased if the background concentration of the tracer gas varies [12]. Considering the time duration of the tracer decay from minutes to few hours [11], this assumption is quite realistic for the CO₂ tracer gas if the air comes directly from the outside. This is an issue, though, for in-situ dwellings applications if the measurement is done in service rooms. The background concentration would be the concentration of the air coming from other rooms, and this concentration is likely to vary depending on CO₂ sources present inside the dwelling.

1.3. Objectives

The purpose of the present paper is to test the robustness of a measurement protocol that adapts the single zone-restricted CO₂ decay method to multi-zone dwellings. Unlike conventional tracer gas methods, this protocol allows assessing the unbiased dynamic global airflow-rate of a passive stack ventilated dwelling. The previous section justified the choice to perform the tracer gas method quasi-simultaneously in service rooms to measure the global airflow-rate, which makes the method sensitive to infiltrations or to a variable background

concentration. To inhibit these sensitivities, the proposed measurement protocol involves both a data pre-treatment procedure that accounts for infiltrations, and the Kalman filter allowing an unbiased dynamic airflow result while the background concentration varies.

The experimental protocol is tested in experimental twincells including a living room and a service room. Variable airflows consistent with natural airflows are imposed by a controllable extract fan in order to assess the robustness of the protocol. Mechanical ventilation allows a reference airflow measurement thanks to conventional airflow-meters. Variable CO₂ background concentration is imposed thanks to occupation in the living room of the twincells. A comparison of the performance of the filter, with the accuracy of the conventional 2-points decay method, is made. Then, the sensitivity towards several parameters is tested, such as occupancy in the living room, position of the door between both rooms, and level of CO₂ injection before the beginning of the decrease.

2. Methods

2.1. Experimental setup

The experiment is performed in a laboratory twincells, composed of two identical zones of 20.4 m³ each. Figure 1 shows a schematic of the experimental cells. The tracer gas measurement is realised in the zone A, which is the room where the airflow is extracted. The door undercut is the only air component, which connects zone A with zone B. In a dwelling, comparable rooms would be service rooms such as the kitchen, toilets, or the bathroom. Zone B contains the air inlet and can be compared to living rooms such as living or bedrooms. The CO₂ tracer gas is injected thanks to a mass-flow controller at a constant rate of 2 L.min⁻¹. 25 minutes of injection allows reaching a concentration around 2500 ppm. A mixing fan is turned on during the injection to ensure homogeneity of the tracer gas before the beginning of the measurement. It is turned off one minute after the end of the injection

period. CO₂ is measured by five auto-calibrated wireless sensors. Their technical specifications are given in Table 1. They form a rectangle in an horizontal plan at 1,3 m. Sensors are not closer to the wall than 50 cm as preconized by Roulet et al. [13]. One sensor is placed at the centre of the rectangle. A sixth sensor is installed in room B, near the door undercut. As the air is distributed from room B, this sensor will provide the measurement of the ambient concentration, described in the previous section. The acquisition frequency of CO₂ sensors is about one measurement every 20 seconds.

Room A is equipped with a mechanical controllable extract fan, that allows to reproduce airflows consistent with natural airflows. The choice of the airflow variation profile is discussed in paragraph 2.3. A mechanical ventilation system was used to allow an accurate direct measurement of the airflow rate, providing the reference airflow value. The airflow-meter used for this measurement is based on the Pitot tube technology. Its technical specifications are also given in Table 1. This measured AER is, then, compared to the AER calculated by tracer gas methods.

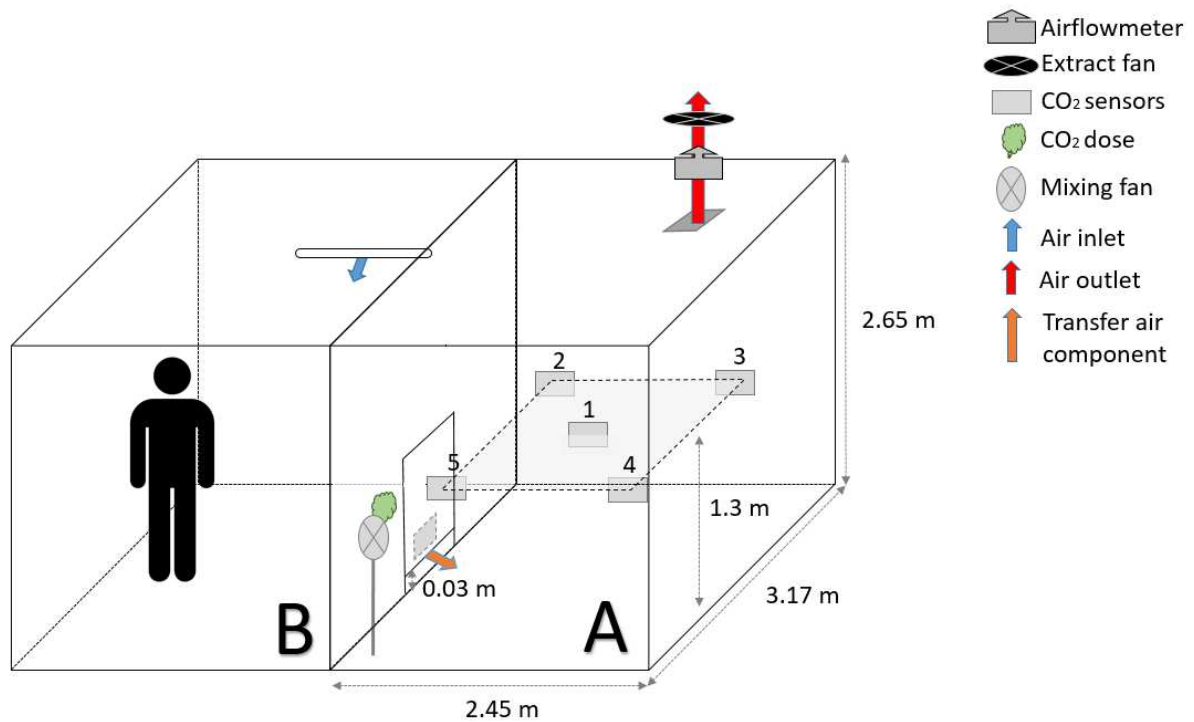


Figure 1 : Schematic of the experimental cell

Table 1 : Technical specifications of the instrumentation

	Technology	Range	Accuracy	Repeatability	Response Time
CO2 sensors	NDIR ¹	0 – 5000 ppm	50 ppm + 3% reading	5% of range/5 years	2 min
NZP1000 Series Nozzle Pitot Airflow sensor	Pitot tube	27,5 – 945 m ³ /h	0,5% of the Flow	0,1% of the Flow	

2.2. Kalman filter

2.2.1. Introduction of the Kalman filter

The Kalman filter is an excellent tool to model dynamic state-space altered by measurement noise. The Kalman filter has already proven twice its efficiency in measuring dynamic airflow

rate [14], [15]. Brabec & Jilek used the Kalman filter to estimate simultaneously the radon entry rate and the AER in a naturally ventilated building [14]. Duarte et al. tested the Kalman filter from CO₂ concentration measurements in classrooms [15]. The Kalman filter was thus used in the so called “transient mass balance equation metabolic CO₂” method [16]. The Kalman filter allowed to simultaneously estimate the natural airflow rate, and the metabolic CO₂ emission rate. In both studies, the Kalman filter appeared to be very interesting for the measurement of natural dynamic airflows [14], [15]. However, the performance of the filter was estimated by analysing the standard-deviation of the state space estimator, which is calculated by the filter. As far as authors know, the Kalman filter has never been compared to a reference airflow on experimental conditions, specifically because it was tested on natural ventilation conditions.

2.2.2. Principle of the Kalman filter

The Kalman filter is a powerful signal processing tool used in several fields of physics. It calculates the state of a dynamic system from noise-corrupted observation series. In our case, the dynamic system encompasses the three parameters involved in the mass balance equation of the tracer gas, namely the background and the inside concentrations, as well as the AER. Noise-corrupted observations are measurements of both concentrations. The interesting thing with the Kalman filter lies in the possibility to determine a covariance matrix that represents the uncertainty in the evolution of parameters of the system that are not predicted by analytical formulas. This covariance matrix is called the process noise covariance matrix. In our case, the analytical formula is the mass balance equation, and its analytical solution would imply:

- A stationary AER;
- A stationary background concentration;

- A perfect mixing of the air;
- An homogeneous tracer gas concentration.

The Kalman filter, using the so-called process noise variance matrix, takes deviations from these assumptions that may occur into account, when correcting the measured concentrations and calculating the state of the dynamic system.

The filter operates through two distinct stages, namely the predicting stage, and the updating stage. The predicting stage uses the estimation of the state-space parameters (concentrations and AER) at the preceding time step to predict the current state-space parameters. Then, predicted state-space parameters are compared to noise corrupted observations, and the filter corrects the state-space parameters knowing the measurement covariance matrix, and the process noise covariance matrix. This stage is called the updating stage. Using only the preceding state to calculate the following makes this filter a recursive filter.

The Kalman filter requires the system to be represented as a state-space model. It means that the system can be formulated as follows:

$$\begin{cases} \dot{x} = A x + B u \\ y = D x + F u \end{cases} \quad (1)$$

The development of the generic formulation of the state-space representation is given in Ref. [15]. It also gives the mathematical development of the Kalman filter. In our case, the state-space representation of the dynamic system is given by the following system of equation, with process noises of the background concentration $\omega_{C_{bg}}$ and the airflow-rate ω_{λ} characterizing their only variation:

$$\left\{ \begin{array}{l} \begin{array}{l} \frac{dC(t)}{dt} \\ \frac{d\lambda(t)}{dt} \\ \frac{dC_{bg}(t)}{dt} \end{array} = \begin{bmatrix} -\lambda & 0 & \lambda \\ 0 & 0 & 0 \\ 0 & 0 & 0 \end{bmatrix} \begin{bmatrix} C \\ \lambda \\ C_{bg} \end{bmatrix} + \begin{bmatrix} 1 & 0 & 0 & 0 & 0 & 0 \\ 0 & 1 & 0 & 0 & 0 & 0 \\ 0 & 0 & 1 & 0 & 0 & 0 \end{bmatrix} \begin{bmatrix} \omega_c \\ \omega_\lambda \\ \omega_{C_{bg}} \\ v_c \\ v_\lambda \\ v_{C_{bg}} \end{bmatrix} \\ \\ \begin{array}{l} C^* \\ \lambda^* \\ C_{bg}^* \end{array} = \begin{bmatrix} 1 & 0 & 0 \\ 0 & 0 & 0 \\ 0 & 0 & 1 \end{bmatrix} \begin{bmatrix} C \\ \lambda \\ C_{bg} \end{bmatrix} + \begin{bmatrix} 0 & 0 & 0 & 1 & 0 & 0 \\ 0 & 0 & 0 & 0 & 0 & 0 \\ 0 & 0 & 0 & 0 & 0 & 1 \end{bmatrix} \begin{bmatrix} \omega_c \\ \omega_\lambda \\ \omega_{C_{bg}} \\ v_c \\ v_\lambda \\ v_{C_{bg}} \end{bmatrix} \end{array} \right. \quad (2)$$

We identify the state-space $x = \begin{Bmatrix} C(t) \\ \lambda(t) \\ C_{bg}(t) \end{Bmatrix}$; the output-space $y = \begin{Bmatrix} C^* \\ \lambda^* \\ C_{bg}^* \end{Bmatrix}$; the command-space

$$\mathbf{u} = \begin{Bmatrix} \omega_c \\ \omega_\lambda \\ \omega_{C_{bg}} \\ v_c \\ v_\lambda \\ v_{C_{bg}} \end{Bmatrix}, \text{ the transition matrix } \mathbf{A} = \begin{bmatrix} -\lambda & 0 & \lambda \\ 0 & 0 & 0 \\ 0 & 0 & 0 \end{bmatrix}, \text{ and the observation matrix } \mathbf{D} =$$

$$\begin{bmatrix} 1 & 0 & 0 \\ 0 & 0 & 0 \\ 0 & 0 & 1 \end{bmatrix}.$$

2.2.3. Measurement noise and process noise covariance matrix

The experimenter has to define the measurement noise and the process noise covariance matrix. The measurement noise covariance matrix was specified by technical specifications provided by the manufacturer:

$$V = \begin{cases} v_c^2 = [(3\% \text{ of reading} + 50)]^2 \text{ ppm}^2 \\ v_{cbg}^2 = [(3\% \text{ of reading} + 50)]^2 \text{ ppm}^2 \end{cases} \quad (3)$$

Concerning the process noise, the one associated with the background concentration and with the internal concentration can be determined by comparison between the filtered and the measured concentrations. An iterative procedure was realised that multiplied both process noise variances until having a good correlation between filtered and measured

concentrations. From process noises of the background concentration and the internal concentration that allowed a good correlation, no influence on the calculation of the AER was experienced by iterating again the procedure. Values of 10 ppm² and 100 ppm², respectively for the inside, and the background concentrations allowed a good filtration of both concentrations for each test presented in this paper.

The main challenging definition of the process noise variance is the one associated with the AER because measurements are not available for graphical. Figure 2 shows the influence of the process noise variance of the AER on the experimental mean deviation and the Root Mean Square Error (RMSE) for one test. Fifty levels of variance values were tested from 0,01 vol².h⁻² to 1 vol².h⁻². From 0,01 to 0,1 vol².h⁻², the experimental mean deviation is decreased by 3 points. Then it reaches an equilibrium mean deviation, which loses 1,5 points until 1 vol².h⁻². In parallel, from 0,01 to 1 vol².h⁻², the RMSE increases from 9,5 to 22%. Figure 3 shows the calculation of the instantaneous AER by the Kalman filter for process noise variances associated with the AER of 0,01, 0,1 and 1 vol².h⁻². The reference airflow measured by the airflow-meter in the extract duct is also plotted. The smallest process noise leads to an inertia that prevents the calculated AER from following the evolution of the reference AER. Increasing the process noise variance of the AER comes down to increase the fluctuations of the calculated AER, as was also described by the increase of the RMSE presented on Figure 2.

For the present experiment, the process noise variance of the AER is set to 0,1 vol².h⁻², as it seems to be a good compromise between both the RMSE and the mean deviation. In real applications with no reference AER, the experimenter should prefer having fluctuations in the calculated AER, rather than having a smoothed curve (see process noise of 0,01 vol².h⁻² on Figure 3). The smoothed curve indicates that the filter's response on the evolution of the airflow rate is not fast enough, risking to deviate from the mean the AER (see small

values of the process noise variance on Figure 2). Observing high frequency fluctuations on the calculated AER does not prevent from under-estimating fluctuations of the real AER; it however prevents from deviating from the mean AER. There is no risk on the mean deviation to over-estimate the process noise variance of the AER as can be seen on Figure 2.

Finally, the covariance matrix of the process noise is defined as follows:

$$R = \begin{cases} r_c = 10 \text{ ppm}^2 \\ r_\lambda = 0.1 \text{ Vol}^2/\text{h}^2 \\ r_{cbg} = 100 \text{ ppm}^2 \end{cases} \quad (4)$$

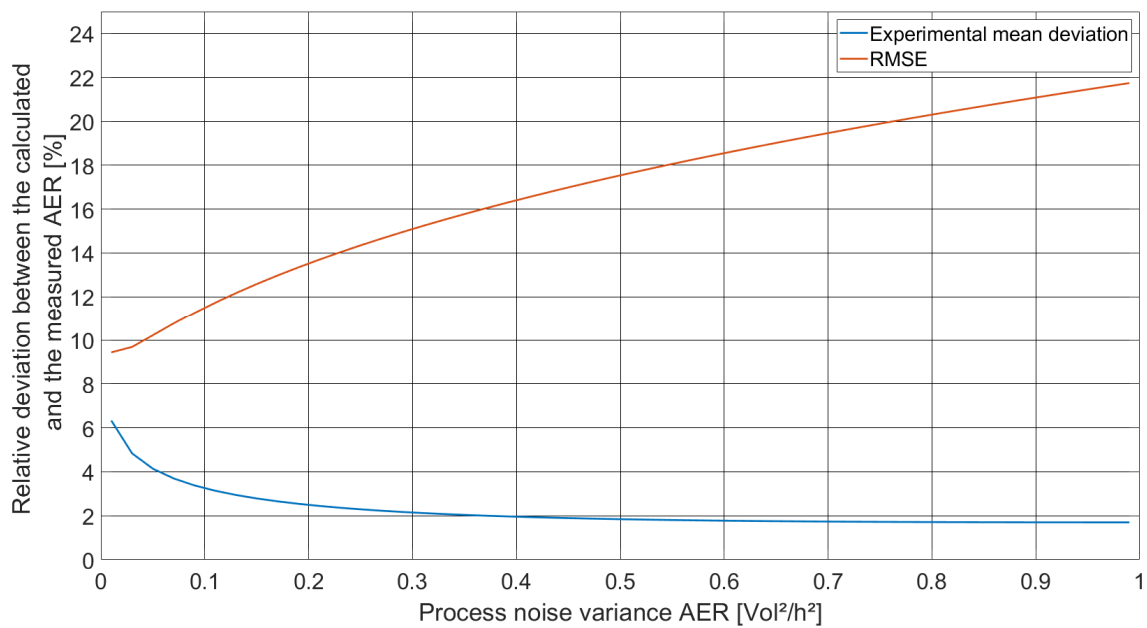


Figure 2 : Influence of the process noise variance of the AER on the relative error

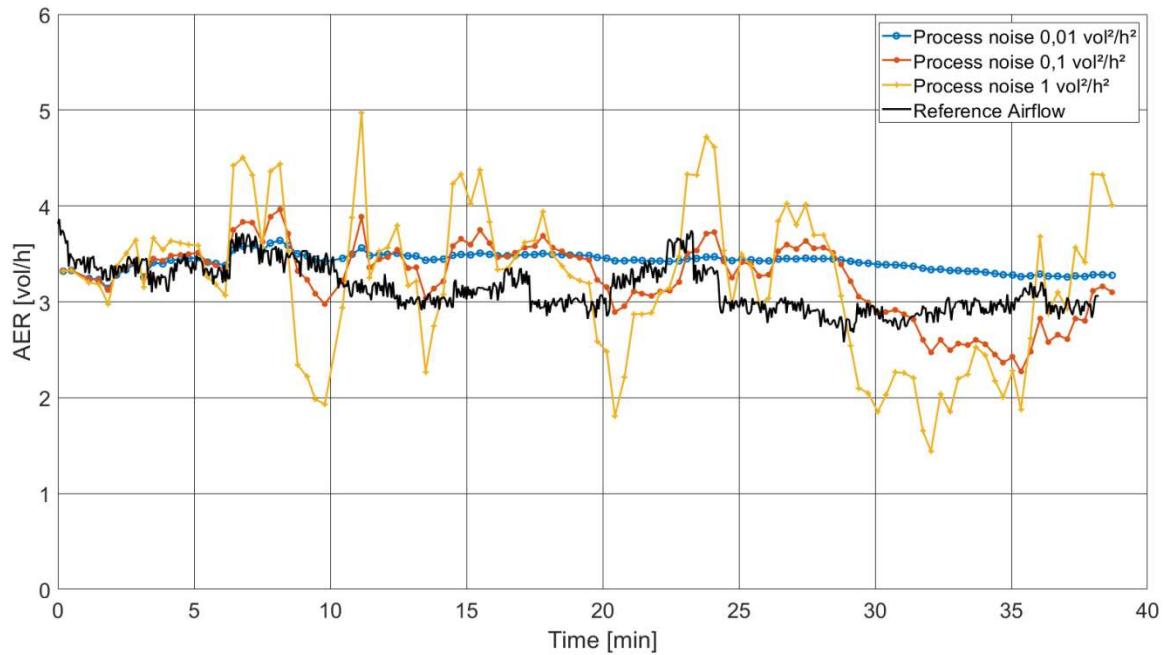


Figure 3 : Instantaneous AER calculation by the Kalman filter with 3 process noise variances of the AER

2.3. Calculation of the AER

Three calculation methods of the AER from the concentration decay are used in this paper. The Kalman filter has been presented in section 2.2. It provides instantaneous results of the dynamic AER. The second and the third calculation methods come from the 2-points decay method, chosen in accordance with prescriptions of the international standard ISO 12569, towards variable airflows [5]. The second method is the conventional 2-points method, and the third represents the 2-points method averaged on five measurement points. This last method will be referred to as “fitted 2-points method”. Both 2-points methods only provide the mean AER between the 2-points that are considered. The first measurement point has to be chosen in order to overcome a transient period following the beginning of the decrease of the gas, where the concentration evolves chaotically [11]. Eight minutes following the end of the injection allowed overcoming this period for each test. The calculation of the AER was performed until two time constants for the comparison between methods to be

representative. Equation 5 gives the formula of the 2-points method [5]. Variation of the background concentration leads to a bias, contrary to the Kalman filter methods:

$$\lambda_2 \cong \frac{1}{t_f - t_i} \cdot \ln\left(\frac{c_f - \overline{c_{bg}}}{c_i - \overline{c_{bg}}}\right) \quad (5)$$

The error propagation law provided an uncertainty of the AER calculated by the 2-points method, evaluated on two time constants, equals to 14,8%.

2.4. Estimation procedure of the background concentration

In dwellings, the air enters from air inlets located in living rooms and flows into the service room thanks to transfer air components, in which it is extracted by an air outlet. Performing the tracer gas test in the service room requires subtracting the background concentration: the concentration of the air flowing to the service room. The measurement of the ambient concentration upstream the transfer air component is not fully representative of the background concentration. Actually, the background concentration is a mixture of the ambient concentration, and of the concentration of any infiltration that may occur from the outside or from an adjacent room to the service room. A procedure is, thus, proposed to correct the ambient concentration in order to take infiltrations into account.

This procedure is based on the assumption that if the entire decrease of the gas is completed, the whole gas has been evacuated and the background concentration at the end should be equal to the inside concentration. The measured ambient concentration should, thus, be corrected in order for these final concentrations to be equal. If insufficient time has been waited, the decrease has not been completed. The procedure takes, then, advantage of characteristic values of the exponential decrease. It is known that after 2 time constants of an exponential decrease, the initial concentration is reduced by 86.5% [11]. Reformulating equation 5, the mean background concentration can be deduced from the inside

concentration only as is shown on equation 6. The measured ambient concentration is, then, corrected by computing equation 7, and becomes the background concentration.

$$\overline{C_{bg}} = \frac{C(2\tau) - C_i}{1 - \exp(-2)} * \exp(-2) \quad (6)$$

$$C_{amb}^*(t) = C_{amb}^*(t) * \left(1 + \frac{\overline{C_{amb}^*} - \overline{C_{bg}}}{\overline{C_{bg}}}\right) \quad (7)$$

In order to identify the period allowing two time constants, the procedure uses the fitted 2-points method. The inside concentration C is first fitted by a moving term average. The procedure is then initialised by computing the fitted 2-points method. The theoretical slope of the decrease is then calculated from the AER. The comparison between the derivate fitted concentration and the theoretical slope allows to identify the two time constants period. Using the theoretical slope instead of the inverse AER allows to reduce the influence of an error in the calculation of the AER. Equations 6 and 7 are then computed, and the procedure is iterated until convergence of the background concentration.

It should be noticed that, based on the exponential decrease of the gas, this procedure is biased if the background concentration varies. If the decrease is complete, correcting the ambient concentration in order to equalize its finale value to the finale inside concentration does not bias the procedure. In our case, the decrease was not completed so the biased procedure was realised. It however, allowed to significantly improve results as will be shown in section 3.3.3. Figure 4 shows an example of the correction of the ambient concentration.

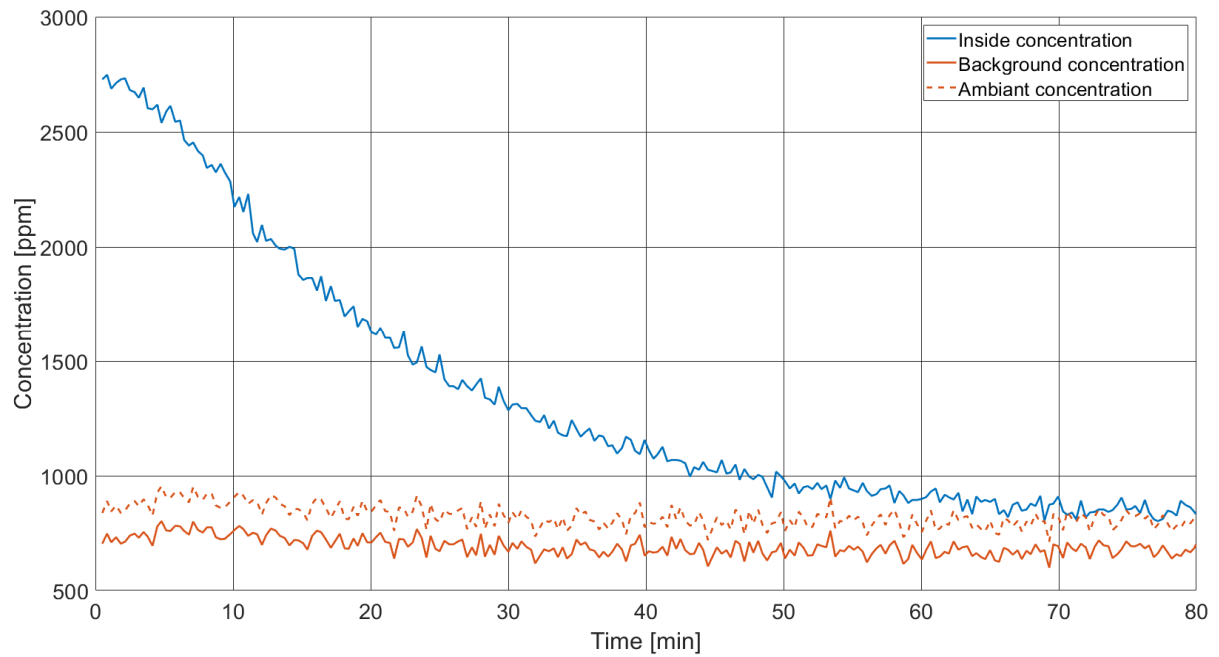


Figure 4 : Concentrations before and after correction

2.5. Definition of the synthetic airflow variation profiles

Airflow variation profiles that were imposed had to be consistent with natural ventilation. Stack ventilation has been selected for the calculation of the synthetic airflow variation profile. It was selected because it is the most represented natural ventilation system of french buildings, especially in existing residential multi-family buildings. The wind was assumed to reinforce airflows induced by buoyancy [17], [18]. Analytical formula given by Hunt et al. have been used to calculate the synthetic AER, from meteorological data of a weather station situated at the roof of the building hosting the experiment, which is located in Lyon France [18] :

$$Q = A_{eff} \cdot \sqrt{u_{buo}^2 + u_{wind}^2} \quad (8)$$

With:

$$u_{buo} = \sqrt{\frac{2 \cdot |\Delta P_{int}|}{\rho_{int}}} = \sqrt{\frac{2 \cdot \rho \cdot g \cdot H \cdot \Delta T}{\rho_{int} \cdot T_{int}}} \quad (9)$$

And:

$$u_{wind} = U \cdot \sqrt{\Delta C_p} \quad (10)$$

We considered for the definition of synthetic AERs a 20 cm² opening in the façade, and a static air extractor of 400 cm² consistent with shunt ducts dimensions. Both discharge coefficients were assumed to have a standard value of 0,6. The height difference between the two openings was equal to 3 meters for the calculation. Meteorological data from a day with a huge amplitude of temperature variation, and a high wind speed were taken. The mean wind speed was equal to 3,5 m.s⁻¹ and the outside temperature had a daily variation amplitude of 10 °C (from 5°C to 15°C). Two periods during the day were isolated to create airflow variation profiles: one decreasing profile in the morning and one increasing in the late afternoon (see Figure 5). Both profiles that were reproduced were 80 minutes long, allowing more than three time constants. Once synthetic profiles have been calculated, the extract fan is controlled by injecting the adequate tension profile from 0 to 10 volts. Figure 5 shows synthetic profiles that were calculated.

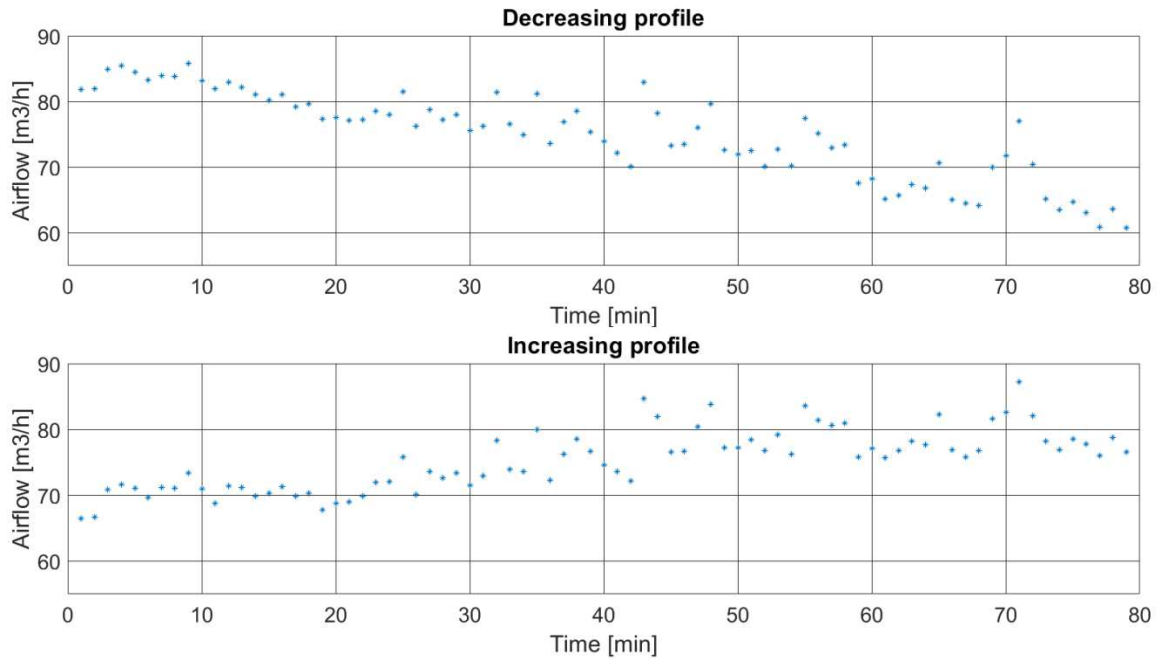


Figure 5 : Synthetic airflow variation profiles consistent with stack ventilation

2.6. Protocol of the experiment

In addition to the comparison of the accuracy of the three methods, a parametric analysis has been realised to assess their sensitivity. Parameters that were chosen for the analysis are:

- Three levels of airflow variations (decreasing, increasing, steady), in order to assess the ability of the Kalman filter to track the evolution of the dynamic AER on different profiles.
- Occupation in the living room (occupied, non-occupied) to verify the insensitivity of the Kalman filter to a variable background concentration.
- The position of the door connecting both rooms (opened, closed) to assess the influence of keeping the door in their usual position for in-situ applications.

- Three levels of initial level of CO₂ injected in the service room A (1500, 2000, 2500 ppm). In-situ applications of the decay method encourage to perform the injection thanks to an impactor that delivers the gas contained in a bottle. The bottle containing the gas has a specific weight so there is an uncertainty in the level that the gas concentration may reach.

The base case is tested through the decreasing airflow variation profile, a closed door between room A and B, and room B not occupied, and an initial level of CO₂ of 2500 ppm. This base case has been repeated 30 times, allowing the assumption that deviations follow a normal distribution. The systematic $\overline{\varepsilon}_\lambda$ and the random errors \overline{S}_ε can be calculated, and the quadratic sum of these two indicators provide the global uncertainty σ_λ of the method (equation 11). The global uncertainty helps to assess the influence of parameters involved in the parametric study. Each other case is repeated three times. Table 2 synthetises this experiment mapping.

$$\sigma_\lambda = \sqrt{\overline{\varepsilon}_\lambda^2 + S_\varepsilon^2} \quad (11)$$

Table 2 : Experiment mapping

Case reference	Profile	Door	Occupation	Initial CO ₂	Number of tests
DCN	Decreasing	Closed	No	2500	30
SCN	Steady	Closed	No	2500	3
ICN	Increasing	Closed	No	2500	3
DCO	Decreasing	Closed	Occupied	2500	3
DOO	Decreasing	Opened	Occupied	2500	3
DON	Decreasing	Opened	No	2500	3

DCNL	Decreasing	Closed	No	1500	3
DCNH	Decreasing	Closed	No	3500	3

Note: To understand the terminology: The first letter refers to the airflow variation profile (Decreasing, Steady, Increasing); The second letter refers to the position of the door (Closed, Opened); The third letter refers to the occupation (Occupied, Non-occupied); The fourth, if it exists, refers to the level of CO₂ injection (Low, High).

3. Results

3.1. Repeatability test and global uncertainty

The 30 tests of base case DCN allowed to assess the repeatability of the Kalman filter method and both 2-points methods (fitted and conventional). The global uncertainty of the three methods were calculated by sensors by computing equation 11. In addition, the spatial sensitivity of the method was assessed by computing the mean standard-deviation between the five sensors' experimental error on the 30 tests. Global uncertainties and spatial standard-deviation are given in Table 3. The 2-points decay method led to an average global uncertainty of 10,6% with a maximum of 13,7%, which is in the 15% range estimated by Remion et al. [3] on a comprehensive study questioning the accuracy of tracer gas methods. On average, the Kalman filter increases the accuracy by 2,3%, while the fitted 2-points method leads to an increase of 3,2% compared to the 2-points method.

Table 3 : Global uncertainty

Method	Global uncertainty $\sigma\lambda$ [%]						Spatial standard-deviation
	Sensor 1	Sensor 2	Sensor 3	Sensor 4	Sensor 5	Average	
Kalman	6,6	8,2	7,8	7,6	11,2	8,3	5,8
Fitted 2-points	6,4	5,3	7,6	7,8	9,9	7,4	7,5

2-points	9,4	6,2	11,8	11,7	13,7	10,6	9,9
-----------------	-----	-----	------	------	------	------	-----

Regarding the spatial standard-deviation, the fitted 2-points method and the Kalman filter reduce the sensitivity by respectively 2,4 and 4,1 points compared to the conventional method. These spatial standard-deviations are below the average global uncertainty, (at 0,1% close for the fitted method) which highlights a weak spatial sensitivity of the three methods. The small volume of the experimental cell can explain this observation. Results from sensor 5 are, however, degraded. Sensor 5 is located on a corner, which is not likely to be in the airstream between the air transfer component and the outlet. The mixing of the air in this particular location is likely to be worse than in other locations.

3.2. Measurement of the dynamic AER by the Kalman filter

One advantage of the Kalman filter compared to the 2-points method is its ability to track the dynamic AER. As was explained in section 2.2, the filter computes the dynamic AER from the filtered concentrations. Figure 6 shows an example of the filtration of concentrations of one test with occupation and door closed (DCO). It can be noticed that the background concentration varies from 875 ppm to 750 ppm in 20 minutes. This variation occurs because of the occupation in the living room.

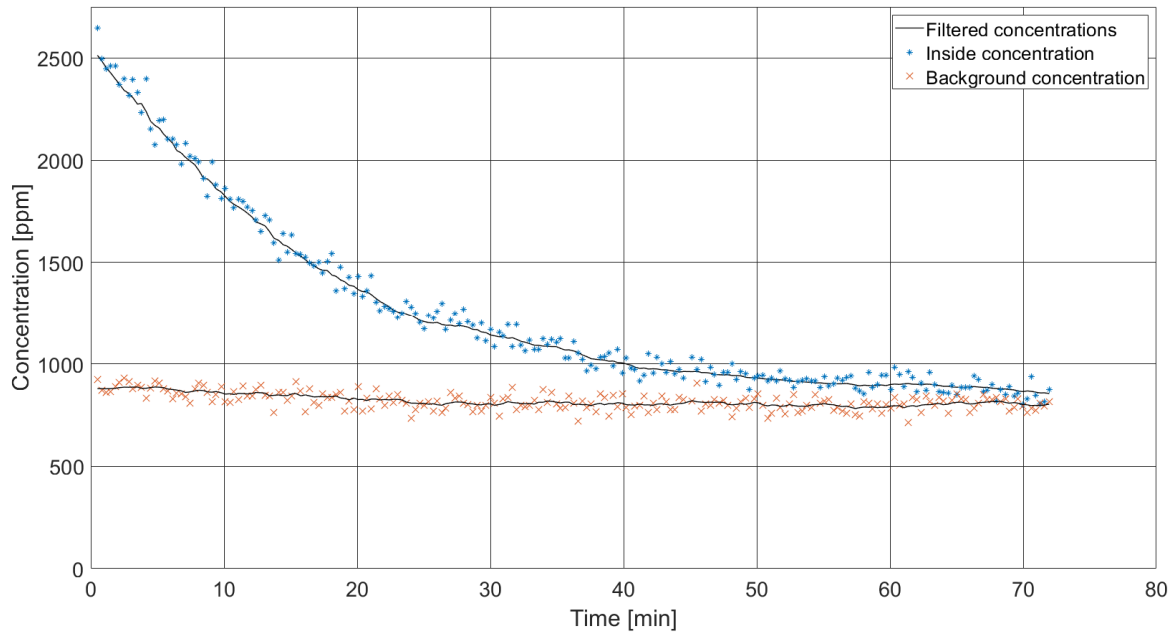


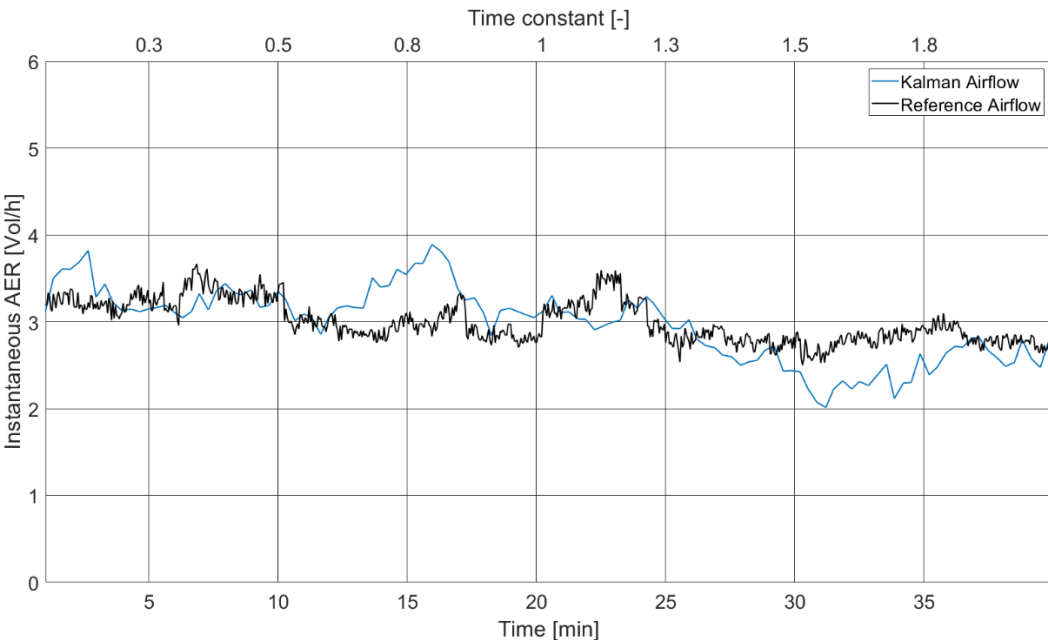
Figure 6 : Filtration of concentrations for one test DCO

Then, the fine tracking ability of the dynamic AER is dependent on:

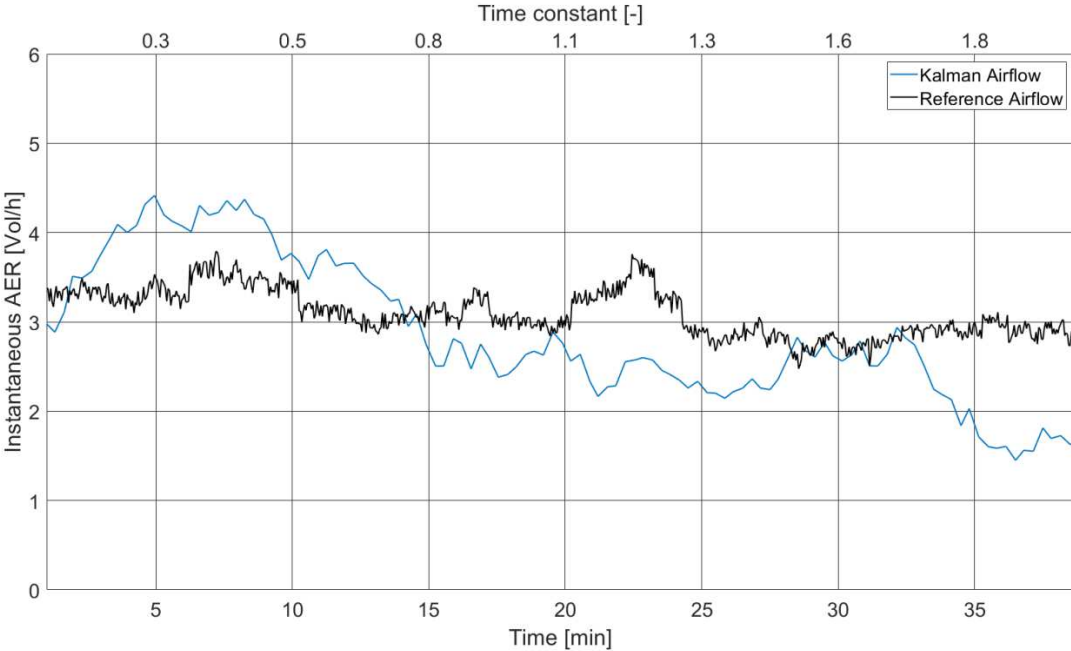
- The good fit between the process noise variance associated with the AER, which is specified in the filter, and the actual variance of the real AER;
- The mixing quality of the fresh air.

Figure 7 gives two examples: one showing a good AER tracking ability of the Kalman filter (i), and another with a weaker correlation (ii). These two tests lead, yet, to a mean deviation on 2 time constants lower than the global uncertainty, respectively 0,8% and 7,3%. (i) is a test of case DCO, and (ii) is a test of case DOO. The most critical case is the case with an opened door between the both zones. The opened door is likely to deteriorate the airflow control, increasing the imperfect mixing, so this is a logical observation. The bad mixing is, here, enhanced by the opened door. However, the mixing of the air in real buildings is not likely to be perfect. As a consequence, coupled with the dependence on the process noise

associated with the AER, the evolution of the dynamic AER should be considered with caution. It, nevertheless, gives an interesting information.



(i)



(ii)

Figure 7 : Example of the AER calculation by the Kalman filter, (i) DCO, (ii) DOO

3.3. Parametric analysis

3.3.1. Comparison between the three tracer gas methods

The parametric analysis aims at assessing the influence of constraints on each method, that in-situ applications may bring. The repeatability test presented in section 3.1 allowed the calculation of each method's global uncertainty on regular conditions. Experimental deviations of each test of the parametric analysis is compared to the global uncertainty, which provides information on the sensitivity of each method. A robust comparison would have require to compute the global uncertainty of each case. The number of 3 tests by case is, however, not enough to assume that experimental deviations follow a normal distribution. The experimental mean deviation and the standard-deviation will be compared individually to the global uncertainty. It provides information about the sensitivity, but conclusions that are drawn have to be further verified. Figure 8 shows the absolute experimental mean deviation for each case. Error bars and crosses represent respectively the standard-deviation, and the maximum deviation for each case. Horizontal lines represent global uncertainties evaluated in paragraph 3.1 for each method. Three tests of the DCN case have been randomly selected among the 30 tests available. Finally, sensor 3 (see Figure 1) located under the outlet has been selected because this location was identified in the literature as being the most representative locations, because the whole gas injected is likely to come by this sensor [2], [19].

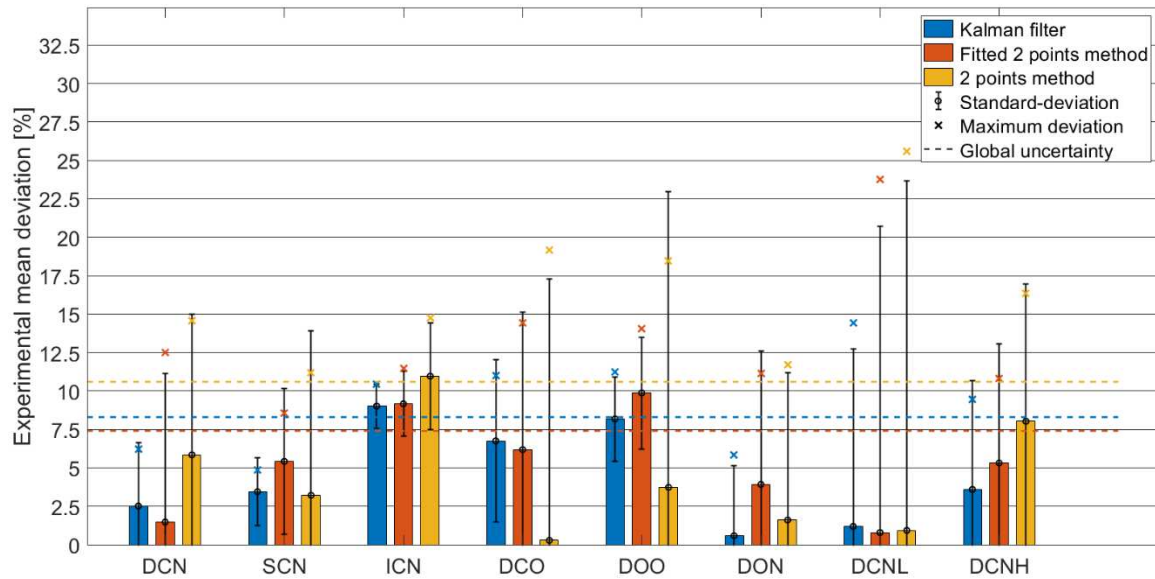


Figure 8 : Histogram of the experimental mean error of both methods

Fitted 2-points, and conventional 2-points methods

Cases SCN, DCO, DOO and DCNL lead to standard-deviations of the 2-points method higher than the global uncertainty of 10,6%, by respectively 1,7%, 17%, 19,2% and 22,7%. In view of its small exceedance, the higher standard-deviation of the case SCN can be attributed to the small number of repetitions. The three other cases involving occupation (DCO, DOO), and a low injection of CO₂ (DCNL) lead to a significant increase of the standard-deviation, with maximum values higher than 18%. It exceeds the usual uncertainty of 15% associated to the 2 points method [3]. The sensitivity towards occupation was expected because the variable background concentration biases the method and Figure 6 showed a variation of the background concentration during the test DCO of 200 ppm. The explanation for the case with a low CO₂ injection (DCNL) could be that measurement uncertainties weigh more on 1500 ppm than on 2500 ppm. More over, the decrease of the gas leads to a faster proximity with the background concentration, which alters the accuracy. Regarding mean deviations, the case with the increasing profile (ICN) only exceeds the

global uncertainty by 0,4%. The case used to compute the global uncertainty involved a decreasing profile. The decreasing profile leads to a lower mean level of CO₂ concentration, as the beginning of the decrease involves higher AER. Measurement uncertainties are proportional, so a higher mean level of CO₂ concentrations means more uncertainties, which can explain the exceedance of 0,4%. We assume that the 2-points method is not sensitive to the airflow variation profile.

Both 2-points methods should lead to the same sensitivity. Results of the fitted method present less risk to be influenced by measurement uncertainties. Among cases that showed an increased sensitivity of the 2-points method (DCO, DOO, DCNL), all of them lead also to an exceedance either of the mean deviation (DOO by 2,5%), or of the standard-deviation (DCO by 1,5%, DCNL by 12,5%). It verifies the sensitivity of both 2-points methods towards a variable background concentration. 2-points methods are also sensitive to a low initial level of CO₂ concentration.

Kalman filter method

The Kalman filter systematically increases the accuracy compared to both 2-points methods. The standard-deviation, and the maximum deviation are always lower. Except case DCNL all other cases lead to standard-deviation lower than the global uncertainty. Case DCNL exceeds the global uncertainty by 3,3%, but the standard-deviation remains significantly lower than 2-points ones by 8,4 and 11,5%. Case ICN only leads to a mean deviation higher than the global uncertainty by 0,8%. It can also be explained by higher measurement uncertainties associated with a higher mean level of CO₂ concentrations (as explained before). The Kalman filter seems insensitive to all parameters that were involved in the parametric analysis, except the low initial level of CO₂. Its sensitivity towards this parameter seems, yet, lower than 2-points methods' one.

3.3.2. *Spatial sensitivity of the Kalman filter*

Sensor 3, which is located near the outlet, was selected for the parametric analysis because it was identified in the literature review as being the most representative [2], [19]. The repeatability case showed that all sensors, except sensor 5, led to similar global uncertainties. The spatial standard-deviation referring to the standard-deviation of the error from the 5 sensors, was evaluated at 5,8%. Some parameters involved in the parametric analysis could increase the spatial sensitivity of the Kalman filter.

Table 4 lists spatial standard-deviations as defined in section 3.1. It also gives the mean deviation of the AER calculated from the averaged concentrations of the 5 sensors. Averaging concentrations from different sensors is usually done to reduce the influence of a bad mixing of the air [20]. The aim is, thus, to assess if results from the averaged concentrations allows to increase the accuracy compared to the sensor located near the outlet considered alone. Values that are given are averaged values of each case.

Among all cases, both cases with the opened door between both cells present a spatial standard-deviation higher than the one evaluated in section 3.1 by 0,8 and 2,8%. This observation is consistent as the opened door is likely to favour the imperfect mixing inside the room. Figure 9 and Figure 10 present the minimum and the maximum AER calculated from individual sensors compared to the reference. Figure 9 lies for a test with a high spatial standard-deviation (one test of the case with the opened door, without occupation DON), while Figure 10 lies for the base case DCN with a low spatial standard-deviation. We can see on Figure 9 a significant discrepancy between the minimum and maximum AER that can be as high as 3 vol.h^{-1} . On the contrary, case DCN leads to discrepancies between sensors that are, most of time, within 1 vol.h^{-1} .

Regarding now the deviation coming from the averaged concentrations between the 5 sensors, it can be seen on Table 4 that averaging concentrations from the 5 sensors increased the accuracy for half of the tests. Deviations associated to these cases coming from sensor 3 alone, though, were not higher than the global uncertainty. However, three cases lead to a higher deviation compared to the global uncertainty (ICN, DCO, DOO), whereas only the first cited case was critical when sensor 3 was considered alone. These deviations exceed respectively by 3,6, 0,4 and 4,2%. Case DOO was already critical in terms of spatial standard-deviation, so the influence of the opened door on the spatial sensitivity is verified. Regarding case DCO, more tests should be conducted to conclude because the deviation is only 0,4 points above the global uncertainty, and can be attributed to the small number of repetitions. Deterioration of case ICN results can possibly be attributed to higher measurement uncertainties, as explained before. Globally, the averaged concentration does not allow an increase of the accuracy compared to the sensor located under the air outlet. A deterioration is even experienced for cases likely to lead to imperfect mixing, or variable background concentration. [2], [19].

Table 4 : Spatial standard-deviation, and mean errors coming from the average of the 5 sensors

	DCN	SCN	ICN	DCO	DOO	DON	DCNL	DCNH
Spatial standard-deviation [%]	2,7	3,1	4,9	4,7	6,6	8,6	3,7	5,7
Deviation from averaged concentration [%]	1,2	-2,3	-11,8	-8,6	-12,4	-1,2	-0,9	1,3

Note : Red values represent either spatial standard-deviation that exceeds the one calculated in the repeatability test (5,8)%; or a deviation from the averaged concentration

higher than the one of sensor 3 alone, as well as the global uncertainty (8,2%). Values in green represent an increase of the accuracy from averaged concentrations.

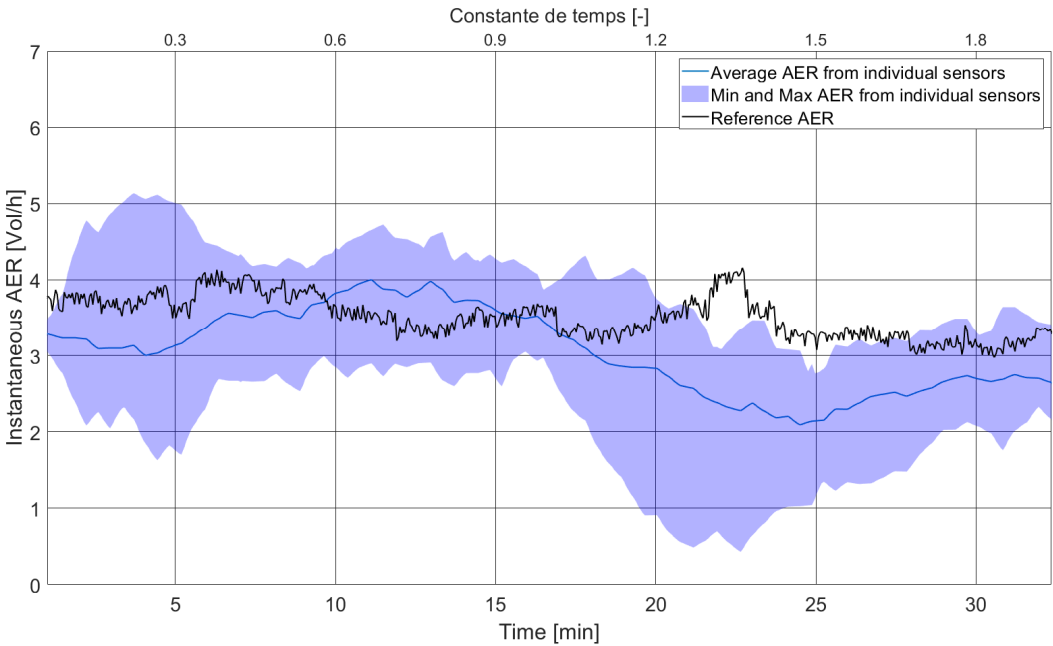


Figure 9 : Minimum and maximum calculated AER of one test DON from the 5 sensors

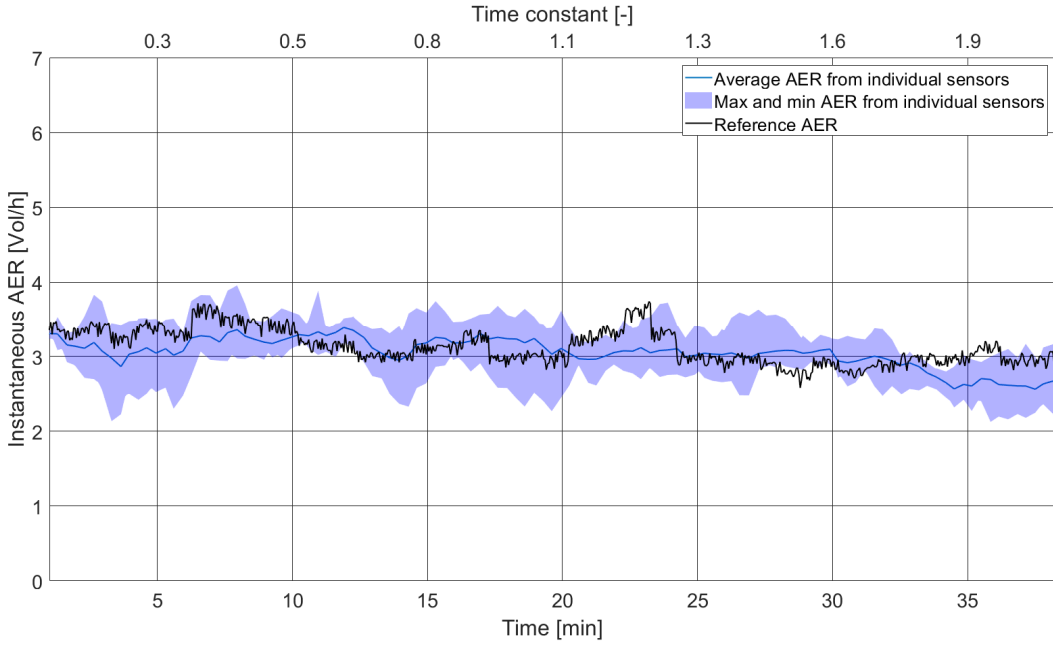


Figure 10 : Minimum and maximum calculated AER of one test DCN from the 5 sensors

3.3.3. Influence of the estimation procedure of the background concentration

Each test of the parametric analysis was also assessed without the application of the estimation procedure of the background concentration described in section 2.4. This procedure intends to correct the measured ambient concentration in the living room, in order to account for infiltrations. The influence of the procedure should, thus, be correlated with the difference between the ambient concentration and infiltrations concentration. The higher is the concentration level inside the building, the more critical should the influence of infiltrations on the calculation of the AER be. Figure 11 shows the correlation between the difference of the deviation for each test with or without application of the procedure, and the level of the measured ambient concentration, without correction. A linear fit was plotted to illustrate the correlation. We can see that for ambient concentrations up to 1000 ppm, the increase of the deviation without application is within 48 and 194%.

For ambient concentrations that are closer from the atmospheric concentration, only one test leads to a lower deviation of 3% without the procedure, four tests lead to a deterioration within 10%, and the twelve remaining tests lead to a deterioration from 10 to 50%.

Infiltrations concentrations, though, should not be too far from the measured ambient concentration, because there were no occupation inside the living room B containing the outside air inlet. The explanation is that a small discrepancy between the calibration of the inside concentration sensor, and the ambient concentration sensor is critical for AER results. The Non-Dispersive Infrared technology involved in a majority of CO₂ sensors is a technology that is likely to deviate in time. An intern calibration procedure is often available within these sensors. This procedure was realised to calibrate each of the sensor used in the present paper. It is convenient but may lead to discrepancies between sensors, compared to certified calibration. What is also interesting with the proposed estimation procedure of the background concentration, is that the measured ambient concentration is corrected

according to the inside concentration only. Yet, it is the evolution of the inside concentration compared to the background concentration, which is at stake, and not their absolute values. The procedure adapts the ambient concentration to the inside concentration, so it means that the application of the estimation procedure inhibits any discrepancy in sensors' calibration, which is very interesting for in-situ applications.

Even if the procedure is biased in case of variable background concentration, it appeared to be robust for each case. It accounts for infiltrations, as well as discrepancies in sensors' calibration. It is an essential step when performing tracer gas methods, with a tracer gas present in the atmosphere, in a multi-zone building.

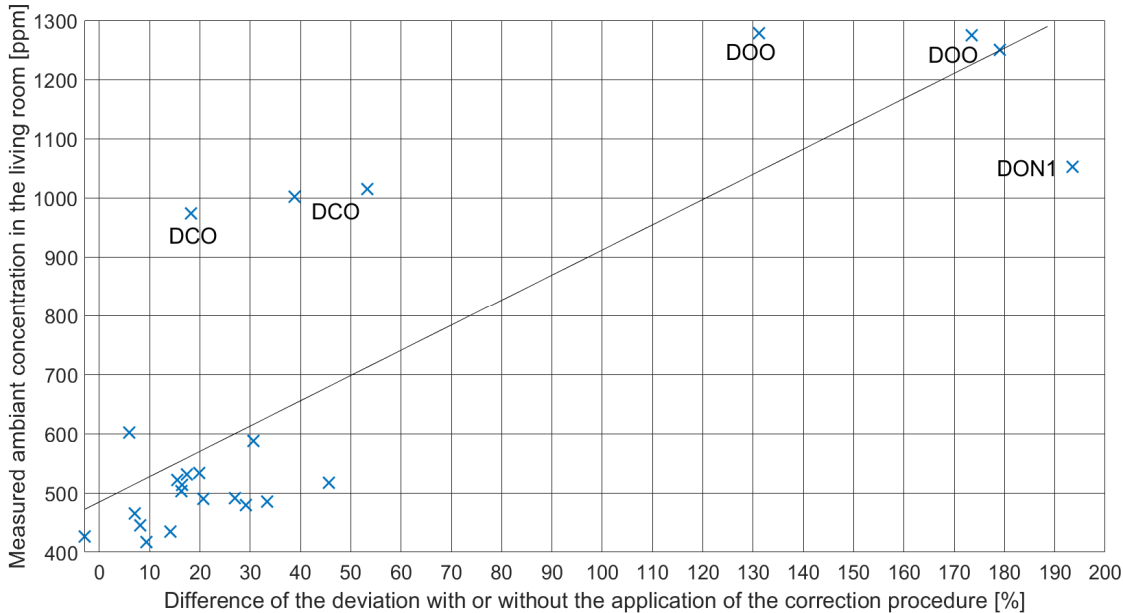


Figure 11 : Correlation between the level of ambient CO₂ concentration and the increase of uncertainty if no procedure is applied

4. Discussion

The Kalman filter appeared to be powerful. The repeatability test on the base case first showed that the Kalman filter and the fitted 2-points method allowed to decrease the global

uncertainty by respectively 2,3 and 3,2%, and the spatial sensitivity by respectively 4,1 and 2,4%. The parametric analysis showed that the Kalman filter was less sensitive than both 2-points methods. It led to mean deviations always lower than its global uncertainty (apart from the case with the increasing profile, which exceeded the global uncertainty by 0,8%). The Kalman filter systematically reduced the standard-deviation, as well as the maximum deviation compared to both 2-points methods. 2-points methods showed an increased sensibility towards occupation and a low initial CO₂ concentration level. The Kalman filter applied to the case with occupation and a closed connecting door, for instance, has reduced the standard-deviation, and the maximum deviation by respectively 4,7 and 2,7% compared to the fitted 2-points method. Regarding the low initial CO₂ concentration level, the filter reduced the standard-deviation of the fitted 2-points method by 8,5%. It is, however, the only case that leads to a standard-deviation of the Kalman filter higher than the global uncertainty. The parameter panel was chosen to assess the influence of constraints that the onsite application may bring. The variable CO₂ concentration induced by occupation can occur inside the building, even if the building is unoccupied during the measurement (if occupants just leaved the building before the beginning of the measurement for example). The initial level of CO₂ is, also, less controlled in in-situ applications, because a mass-flow controller is not always available or adapted. The better performance of the Kalman filter during the parametric study highlights its potential for increasing the reliability of the multi-zone in-situ applications of the decay method. This should be further tested through a higher number of tests, or numerically, to draw solid conclusions. It also has the benefit to track the dynamic AER. However, the dependency of its tracking capacity on the process noise involved in the Kalman filter, and on the mixing quality of the air encourage to consider the dynamic AER with caution.

It is important to question the sensitivity of the conclusions drawn here regarding the process noise covariance matrix involved in the Kalman filter. Regarding the process noise of the inside and the background concentrations, the adequacy of their associated process noise can be verified graphically, by plotting the measured concentrations and the filtered ones. Regarding now the process noise of the AER, the RMSE strongly depends on its value. The mean deviation, however, is little sensitive to the process noise of the AER, as long as it is not under-estimated. In real applications, with no reference, insights regarding the under-estimation of the process noise have to be found. If the process noise of the AER is under-estimated, the evolution of the dynamic AER is smoothed, and rather monotone. It presents a risk that the calculated mean AER deviates from the real mean AER. Observing high-frequency fluctuations on the calculated instantaneous AER, verifies that, at least, the mean calculated AER does not deviate significantly from the real one. There is no risk on the mean deviation to be increased by overestimating the process noise associated to the AER. Thus, the experimenter should observe high frequency fluctuations on the calculation of the AER.

5. Conclusion

Performing the single-tracer gas decay method in dwellings to assess the global AER is not planned by standards describing tracer gas methods. It implies to perform those methods quasi-simultaneously in each service room. CO₂ is a convenient and cost-effective tracer-gas to dose and to monitor. However, if the tracer gas is present in the atmosphere, its background concentration should be measured and subtracted to the inside concentration. The measurement of its background concentration should be done upstream the transfer air component connected to the service room. Any incoming air, which would not flow through this component, such as infiltrations, would significantly affect the tracer gas method. A procedure was proposed to correct the concentration measured upstream of the transfer air component, in order to take infiltrations into account. It also inhibits the effect of

discrepancies in sensors' calibration. This procedure significantly improved results, up to 195 points. It is an essential step when performing a tracer gas method in multi-zone dwellings, with a gas present in the atmosphere.

If the background concentration varies, the decay method is biased. The Kalman filter has been applied on the decreasing concentration to test its ability to calculate the dynamic AER while the background concentration of the tracer gas is varying. In addition to the impact of the variation of the background concentration, the sensitivity towards the position of the door between the service and the living room, as well as the initial level of tracer gas injection has been assessed. On this parametric analysis, the Kalman filter systematically increased the accuracy compared to 2-points decay methods. It allowed to significantly reduce 2-points decay methods' sensitivities towards a variable background concentration induced by occupation, and towards a low initial level of CO₂. It showed its reliability potential for in-situ applications in an occupied passive-stack ventilated dwelling, as long as occupants stay in living rooms. These interesting results have to be further tested through more tests, or through numerical models.

Acknowledgment

The authors would like to thank the French Ministry of Sustainable Development for its financial contributions.

References

- [1] G. Bekö *et al.*, 'Diurnal and seasonal variation in air exchange rates and interzonal airflows measured by active and passive tracer gas in homes', *Build. Environ.*, vol. 104, pp. 178–187, Aug. 2016, doi: 10.1016/j.buildenv.2016.05.016.

- [2] S. Cui, M. Cohen, P. Stabat, and D. Marchio, 'CO2 tracer gas concentration decay method for measuring air change rate', *Build. Environ.*, vol. 84, no. Supplement C, pp. 162–169, Jan. 2015, doi: 10.1016/j.buildenv.2014.11.007.
- [3] G. Remion, B. Moujalled, and M. El Mankibi, 'Review of tracer gas-based methods for the characterization of natural ventilation performance: Comparative analysis of their accuracy', *Build. Environ.*, vol. 160, pp. 106–118, 2019.
- [4] C. Y. Chao, M. P. Wan, and A. K. Law, 'Ventilation performance measurement using constant concentration dosing strategy', *Build. Environ.*, vol. 39, no. 11, pp. 1277–1288, Nov. 2004, doi: 10.1016/j.buildenv.2004.03.012.
- [5] AFNOR, 'NF EN ISO 12569 - Performance thermique des bâtiments et des matériaux - Détermination du débit d'air spécifique dans les bâtiments - Méthode de dilution de gaz traceurs'. AFNOR, 2017.
- [6] ASTM, *ASTM E741 - 00 : Standard Test Method for Determining Air Change in a Single Zone by Means of a Tracer Gas Dilution*. 2000.
- [7] Y. Allab, 'Evaluation expérimentale des performances des systèmes de ventilation dans le bâtiment: efficacité de ventilation et confort thermique', PhD Thesis, Paris, ENSAM, 2017.
- [8] C.-A. Roulet and L. Vandaele, 'Air flow patterns within buildings measurement techniques', AIVC, AIVC Technical Note 34, 1991. [Online]. Available: <https://www.aivc.org/resource/tn-34-air-flow-patterns-within-buildings-measurement-techniques>.

- [9] M. Sandberg, 'What is ventilation efficiency', *Build. Environ.*, vol. 16, no. 2, pp. 123–135, 1981.
- [10] M. Sherman, 'Tracer-Gas Technique For Measuring Ventilation in a Single Zone', *Build. Environ.*, vol. 25, no. 4, pp. 365–374, 1990.
- [11] D. Laussmann and D. Helm, 'Air change measurements using tracer gases: Methods and results. Significance of air change for indoor air quality', in *Chemistry, Emission Control, Radioactive Pollution and Indoor Air Quality*, InTech, 2011.
- [12] J. Dias Carrilho, M. Mateus, S. Batterman, and M. Gameiro da Silva, 'Air exchange rates from atmospheric CO₂ daily cycle', *Energy Build.*, vol. 92, pp. 188–194, Apr. 2015, doi: 10.1016/j.enbuild.2015.01.062.
- [13] C.-A. Roulet, R. Compagnon, and M. Jakob, 'A Simple Method Using Tracer Gas to Identify the Main Airflow and Contaminant Paths within a Room', *Indoor Air*, vol. 1, no. 3, pp. 311–322, Sep. 1991, doi: 10.1111/j.1600-0668.1991.08-13.x.
- [14] M. Brabec and K. Jílek, 'State-space dynamic model for estimation of radon entry rate, based on Kalman filtering', *J. Environ. Radioact.*, vol. 98, no. 3, pp. 285–297, Dec. 2007, doi: 10.1016/j.jenvrad.2007.05.006.
- [15] R. Duarte, M. Glória Gomes, and A. Moret Rodrigues, 'Estimating ventilation rates in a window-aired room using Kalman filtering and considering uncertain measurements of occupancy and CO₂ concentration', *Build. Environ.*, vol. 143, pp. 691–700, Oct. 2018, doi: 10.1016/j.buildenv.2018.07.016.

- [16] S. Batterman, 'Review and Extension of CO₂-Based Methods to Determine Ventilation Rates with Application to School Classrooms', *Int. J. Environ. Res. Public Health*, vol. 14, no. 12, p. 145, Feb. 2017, doi: 10.3390/ijerph14020145.
- [17] B. Wang, D. W. Etheridge, and M. Ohba, 'Wind tunnel investigation of natural ventilation through multiple stacks. Part 1: Mean values', *Build. Environ.*, vol. 46, no. 7, pp. 1380–1392, Jul. 2011, doi: 10.1016/j.buildenv.2011.01.007.
- [18] G. R. Hunt and P. P. Linden, 'The fluid mechanics of natural ventilation—displacement ventilation by buoyancy-driven flows assisted by wind', *Build. Environ.*, vol. 34, no. 6, pp. 707–720, Nov. 1999, doi: 10.1016/S0360-1323(98)00053-5.
- [19] S. Van Buggenhout, A. Van Brecht, S. E. Özcan, E. Vranken, W. Van Malcot, and D. Berckmans, 'Influence of sampling positions on accuracy of tracer gas measurements in ventilated spaces', *Biosyst. Eng.*, vol. 104, no. 2, pp. 216–223, 2009.
- [20] M. Sandberg and C. Blomqvist, 'A quantitative estimate of the accuracy of tracer gas methods for the determination of the ventilation flow rate in buildings', *Build. Environ.*, vol. 25, no. 4, pp. 139–150, 1985.